ELSEVIER

Thermochimica Acta 380 (2001) 5–12

thermochimica acta

www.elsevier.com/locate/tca

Step response analysis in DSC — a fast way to generate heat capacity spectra

M. Merzlyakov, C. Schick*

Department of Physics, University of Rostock, Universitätsplatz 3, D-18051 Rostock, Germany

Received 8 March 2001; received in revised form 7 June 2001; accepted 11 June 2001

Abstract

A new method of step response analysis in DSC was developed which allows the fast generation of heat capacity spectra. In common temperature modulated calorimetry, like 3ω-method, AC-calorimetry and temperature modulated differential scanning calorimetry (TMDSC), periodic perturbations are used to get dynamic heat capacity. In contrary, the proposed method uses a single step in program temperature followed by an isothermal segment to obtain the spectrum of heat capacity. To follow system evolution with time or temperature, one can repeat the temperature step, like in StepScan-DSC™ (PerkinElmer Instruments), several times also in a non-periodic manner. Measured heat flow rate is evaluated in time domain. With this method, it is possible to cover more than two orders of magnitude in frequency in a single measurement. This allows a dramatic shortening of the measuring time compared to TMDSC. A linearity check and the comparison with TMDSC results are presented. Complete data analysis is performed by a software available for download from our website.

Keywords: DSC; Complex heat capacity; Step response; Heat capacity spectrum

1. Introduction

In differential scanning calorimetry (DSC), one commonly measures the heat flow rate into the sample under non-zero heating/cooling rate, i.e. under scanning of temperature. In general case, the relation between heating rate and heat flow rate can be very complicated. Under linear and stationary thermal response, this relation is described by a convolution product. There are two ways to resolve the convolution product: either to use Fourier or Laplace transformation. Temperature modulated DSC (TMDSC), introduced first time by Gobrecht et al. [1], applies periodic temperature oscillations to the system and analyzes amplitude and phase of the corresponding periodic heat flow rate. The measured signals are Fourier transformed to obtain dynamic heat capacity c_p^* which equals the ratio between heat flow rate amplitude and heating rate amplitude. The value of c_p^* often depends on frequency of temperature modulation. The detailed study of the c_p^* spectrum is very informative since it contains almost all information about the measured system which one can get by analyzing the heat flow rate. The c_p^* spectrum can be used for studying dynamic glass transition [2], kinetics of irreversible and reversible processes [3–5], for determination of the accurate value of heat capacity [6] and the thermal conductivity [7].

* Corresponding author. Tel.: +49-381-498-1644; fax: +49-381-498-1626.
E-mail address: christoph.schick@physik.uni-rostock.de (C. Schick).

0040-6031/01/$ – see front matter
PII: S0040-6031(01)00631-1

Another way to resolve the complicated relation between the heat flow rate and the heating rate is the analysis in time domain of a heat flow rate as a response on a step perturbation. To the best of our knowledge, the first stepwise method for differential thermal analysis (DTA) was introduced by Staub and Perron [8]. In their ''step heating programming technique'', the temperature is increased stepwise; the heat flow peak after the temperature step is integrated in time domain to determine the enthalpy changes, which corresponds to the temperature increase. This integral value equals the Laplace transformed heat flow with the variable set to zero. However, relaxation times and spectra were not evaluated by these authors. Such methods are in use for purity determination and in the PerkinElmer Instruments StepScan^{TM}-DSC software for heat capacity measurements.

Schawe et al. [9,10] proposed a method to measure the dynamic behavior of DSC instruments by steps in heating rate (switching from isotherm to heating with constant heating rate and switching from heating to isotherm, respectively). The apparatus function, which is calculated by applying Laplace transformation to the heat flow rate just after switching, describes the dynamic behavior of the instrument and how the measured signal is smeared. This apparatus function is used to desmear the whole measured heat flow signal.

Agarwal and Farris [11,12] proposed the pulsed DSC method, where an input pulse of temperature is applied to the system and the output heat flow rate is collected. Essential point of the method is that both the input and output must return to their initial unperturbed state at the end of the experiment. A simple Laplace analysis of the input and output data yields the equilibrium specific heat and a mean relaxation time, whereas the frequency dependent quantities are calculated by Fourier transform [11].

We present another method of generating frequency dependent quantities by DSC where the programmed temperature undergoes a sharp single step followed by an isothermal segment. To follow system evolution with time or temperature, one can repeat the temperature step, like in StepScan-DSC^{TM} (PerkinElmer Instruments), several times also in a non-periodic manner. Measured heat flow rate is evaluated in time domain by Laplace transformation to obtain the heat capacity spectrum. For better understanding of how the method works, why it gives the right heat capacity spectrum and what are the limitations, we first review the data treatment of classical TMDSC method [1] and that of multi-frequency TMDSC [13] and present the data treatment which can be applied to a single step analysis. This is done in Section 2. Next, we show two examples how to perform the step analysis measurement. After that, in Section 4, we demonstrate how a linearity check can be performed and compare the results from the step response analysis with that from classical TMDSC. In Section 5, we show how to measure c_p^* spectrum even faster depending on sample response. Finally, in Section 6, we compare the presented method with other possible ways to generate heat capacity spectra.

2. Data treatment

2.1. TMDSC

Gobrecht et al. [1] added an alternating current to the reference current of temperature control of power compensated DSC. One should note that to determine the amplitude of a heat flow rate was not a simple task. They realize mechanically a lock-in technique and calculate in-phase and quadrature components of a heat flow rate I_{Re} and I_{Im}, respectively (phase shift is determined with respect to periodic temperature of the sample holder). Further, they determine a complex thermal admittance $Y = G + iB$ as $G = \pi I_{Re}/2At$ and $B = \pi I_{Im}/2At$, where A is the temperature amplitude, t the integration time of I_{Re} and I_{Im}. From complex thermal admittance of network of heat capacities, they determine the complex heat capacity consisting of two parts: a vibrational part C_{vib} showing no relaxation behavior, and a configuration part C_{con}, which relaxes with a time constant τ [1].

In fact $\pi I_{Re}/2t$ equals $A_{HF\,Re}$ and $\pi I_{Im}/2t$ equals $A_{HF\,Im}$, where $A_{HF} = A_{HF\,Re} + iA_{HF\,Im}$ is the heat flow rate amplitude. Therefore, complex thermal admittance is determined as $Y = A_{HF}/A$. On the other hand, $Y = i\omega C_{eff}(\omega)$, where $C_{eff}(\omega)$ is an effective (apparent) heat capacity of the measured system (a network of heat capacities), which reads:

$$C_{eff}(\omega) = \frac{A_{HF}(\omega)}{i\omega A} = \frac{A_{HF}(\omega)}{A_q(\omega)}, \quad (1)$$

where $A_q(\omega)$ is a heating rate amplitude.

One can further calculate from that value the true sample heat capacity by means of a calibration procedure [14] but it is not an essential point for our consideration here. The important point is that the heat capacity at frequency ω can be calculated only at a non-zero heating rate amplitude, $A_q(\omega)$, which means that the heating rate $q(t)$ should have a periodic component with frequency ω. If the instrument has such a sampling rate that we get n points per period for HF(t) and $q(t)$ signals, then Eq. (1) can be rewritten as

$$C_{\mathrm{eff}}(\omega) = \frac{\sum_{i=1}^{n} \mathrm{HF}_i \cos(\omega t_i) - \mathrm{i}\sum_{i=1}^{n} \mathrm{HF}_i \sin(\omega t_i)}{\sum_{i=1}^{n} q_i \cos(\omega t_i) - \mathrm{i}\sum_{i=1}^{n} q_i \sin(\omega t_i)}. \tag{2}$$

2.2. Single step analysis

As shown in [13], the periodic heating rate $q(t)$ should contain a delta function to generate an uniform heat flow rate spectrum (that is equal to $A_q(\omega_k)$ at different frequencies $\omega_k = k\omega_0$, $\omega_0 = 2\pi/t_\mathrm{p}$, t_p is the basic period of $q(t)$, k the integer). Then the temperature–time profile should have infinite sharp stepwise changes. Let us consider a single period of such a heating rate function together with the respective heat flow rate as shown in Fig. 1a.

If the period between pulses is long enough, then the heat flow rate reaches the steady state value before the next temperature step. Since the heat flow rate is periodic, each peak in the heat flow rate starts from the same steady state value. We can set the steady state value of the heat flow rate to zero without influencing the amplitudes of all harmonics. The same we can do with the heating rate.

Since we have a steady state part of the heat flow rate before the peak, the peak itself does not "feel" the previous peaks. Consequently, the shape of the peak is exactly the same as that of a single peak measured with only one heating rate pulse, see Fig. 1b. We can treat this single peak as a single period of some fictitious periodic function with basic period t'_p or t''_p, see Fig. 1c, and calculate $C_{\mathrm{eff}}(\omega)$ at the set of frequencies $\omega'_k = k2\pi/t'_\mathrm{p}$ or $\omega''_k = k2\pi/t''_\mathrm{p}$. The shortest possible basic period $t_{\mathrm{p\,min}}$ of such a function is the time the heat flow rate returns back to the steady state value after the perturbation. The longest basic period $t_{\mathrm{p\,max}}$ is the time interval the heat flow rate has been actually measured after the temperature step. Since we can vary the basic period in a certain range for this single step in temperature, we generate a continuous spectrum of heating rate instead of a discrete spectrum in case of the periodic $q(t)$. Then $C_{\mathrm{eff}}(\omega)$ can be calculated for a continuous frequency range $\omega \geq 2\pi/t_{\mathrm{p\,max}}$.

We can start the Fourier integration just at the position of the delta function (for real measurements — at the beginning of the temperature step) and

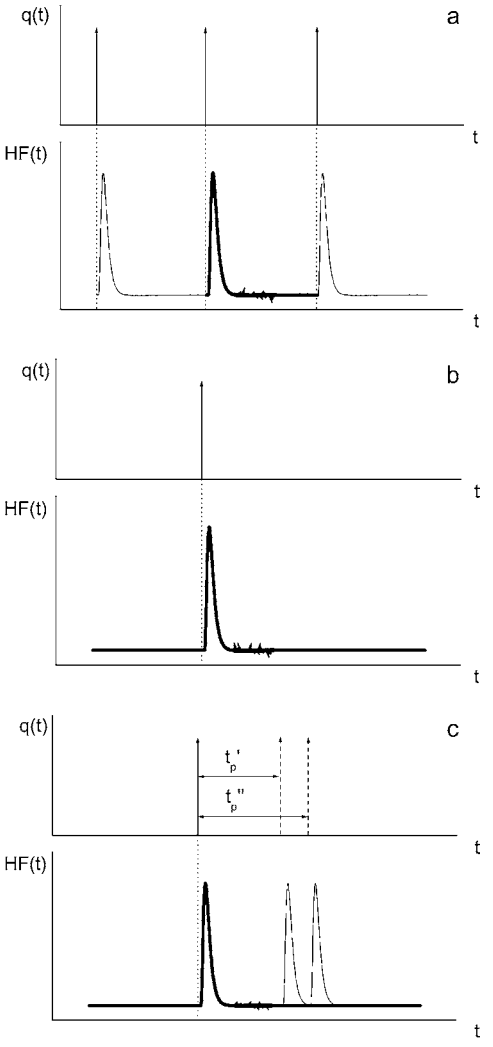

Fig. 1. Heating rate $q(t)$ as a delta function and the corresponding heat flow rate HF(t) for periodic heating rate (a), single heating rate pulse (b), single heating rate pulse, which can be followed by another pulse after the time interval t'_p or t''_p (c).

integrate over the whole period t'_p or t''_p. In fact, heat flow rate does not contribute to the Fourier integral any more after its relaxation back to the steady state value. Then the only variable for $C_{eff}(\omega)$ determination is the frequency ω.

Finally, the data treatment becomes nothing else as an operational calculus. The complicated relation in time domain between heat flow rate and heating rate, which is given by a convolution product, can be resolved using the Laplace transformation $L(p) = \int_0^{+\infty} f(t)\, e^{-pt}\, dt$, where variable p can be any complex number and $f(t)$ represents heating rate $q(t)$ and heat flow rate HF(t). We can set $p = i\omega$ and choose the time scale so that $t = 0$ at the very beginning of the temperature step. We calculate Laplace transformation of the heating rate $q(t)$ and the heat flow rate HF(t) as

$$L(i\omega) = \int_0^{+\infty} f(t)\, e^{-i\omega t}\, dt = \int_0^{t'_p} f(t)\, e^{-i\omega t}\, dt \qquad (3)$$

because remaining integral $\int_{t'_p}^{+\infty} f(t)\, e^{-i\omega t}\, dt$ equals zero for both $q(t)$ and HF(t) (remember that we set the steady state values of $q(t)$ and HF(t) to zero by subtracting the constant offset values). We can determine the effective heat capacity as follows:

$$C_{eff}(\omega) = \frac{\int_0^{t'_p} HF(t)\, e^{-i\omega t}\, dt}{\int_0^{t'_p} q(t)\, e^{-i\omega t}\, dt}. \qquad (4)$$

We fix the integration limits and vary only the frequency ω to get the heat capacity spectrum. If we sample n points of heat flow rate and of heating rate during the time interval $(0, t'_p)$, the integrals can be changed to sums and Eq. (4) equals exactly Eq. (2), since $e^{-i\omega t} = \cos(\omega t) - i\sin(\omega t)$. Further for real measurement, we use Eq. (2).

The area under the heat flow rate peak in time domain is the total amount of heat absorbed by the sample due to the stepwise increase of temperature. This heat equals the numerator in Eq. (4) for $\omega = 0$, that is then simply integral $\int_0^{t'_p} HF(t)\, dt$, and the height of the temperature step equals the denominator. Therefore, $C_{eff}(0)$, calculated by Eq. (4) or Eq. (2) for $\omega = 0$, corresponds to the total heat capacity.

Presented data treatment can be performed by a software package available for download from our website (see [15]).

3. How to perform the measurements?

As we see from previous section, the single step measurement can be analyzed as a fictitious periodic measurement under the condition that $q(t)$ and HF(t) start and end at the same steady state values. Therefore, to get correct $C_{eff}(\omega)$ values by Eq. (2), the measurements should start from steady state. The step in temperature can be approximated as a very steep heating (or cooling) ramp in short time. In the examples shown in Figs. 2 and 3, we used a programmed heating rate of 75 K/min for 0.8 and 1.6 s to have 1 and 2 K temperature steps, respectively. After the temperature step the heat flow rate HF(t) should be recorded until it returns back to steady state.

As one can see from both figures the measured step in the temperature–time profile is not as sharp as it was programmed because of instrumental delay. The power compensated system (Fig. 2), having much smaller furnaces than the heat flux system (Fig. 3), responds much faster and follows more tightly the program temperature (note the difference in the time scale in both figures). For $C_{eff}(\omega)$ determination by Eq. (2), a large part of the instrumental delay can be eliminated by using the measured heating rate instead of the programmed one.

$C_{eff}(\omega)$ values, calculated by Eq. (2) correspond to some average values of actual $C_{eff}(\omega)$ spectrum in the temperature range $(T_0,\ T_0 + \Delta T)$ and in the time interval $(t_0,\ t_0 + t_{p\,max})$, where T_0 is the starting temperature of the step measurement, ΔT the height of the temperature step, t_0 the starting time, $t_{p\ max}$ the total measuring time of the single step. If one further wishes to monitor the evolution of the $C_{eff}(\omega)$ spectrum with changing temperature or with time (e.g. during isothermal crystallization), one can repeat the step perturbation at another temperature or at another time.

4. Linearity check and comparison with TMDSC results

To compare the results from this step analysis with that from classical TMDSC, we took two extreme cases of a very good heat conducting sample with small mass and another larger and poor heat conducting sample. A thin aluminum disk (with 0.25 mm thickness and 16 mg mass) and a thick polystyrene

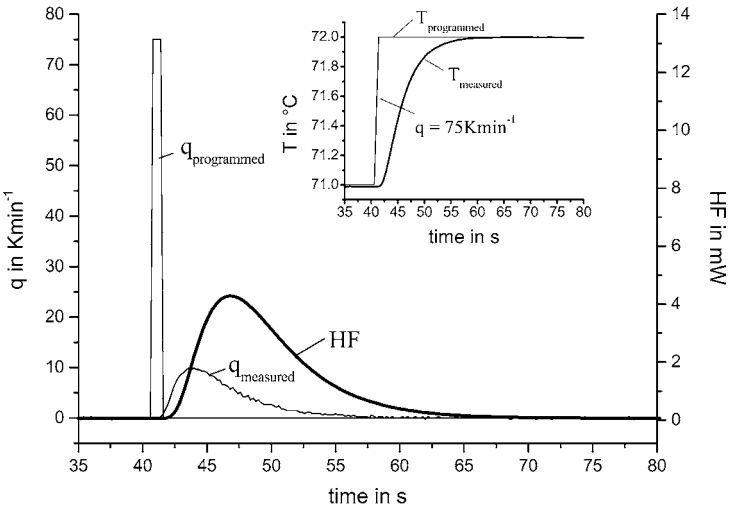

Fig. 2. Heating rate $q_{\text{programmed}}(t)$ and $q_{\text{measured}}(t)$ and heat flow rate HF(t) versus time for one temperature step. The insert shows programmed and measured temperature, $T_{\text{programmed}}$ and T_{measured}. Heating rate is calculated as time derivative of temperature. PerkinElmer Instruments Pyris-1 DSC, polystyrene $m_s = 27$ mg.

disk (2 mm, 56 mg) were measured with the following temperature–time profile consisting of two heating and two cooling steps with 1 and 2 K heights, see Fig. 4.

Both the samples were measured directly in the DSC furnace without a pan. Just after the step measurement, without changing the sample, six standard TMDSC measurements were performed with periods of 4 min, 2 min, 1 min, 30 s, 15 s and 7.5 s and with programmed heating rate amplitude $A_q(\omega) = 2\,\text{K}/\text{min}$. At the longest period (4 min) of the TMDSC measurements, the peak-to-peak temperature amplitude was about 2 K — the same as in the large cooling and heating steps. After sample runs, a baseline run

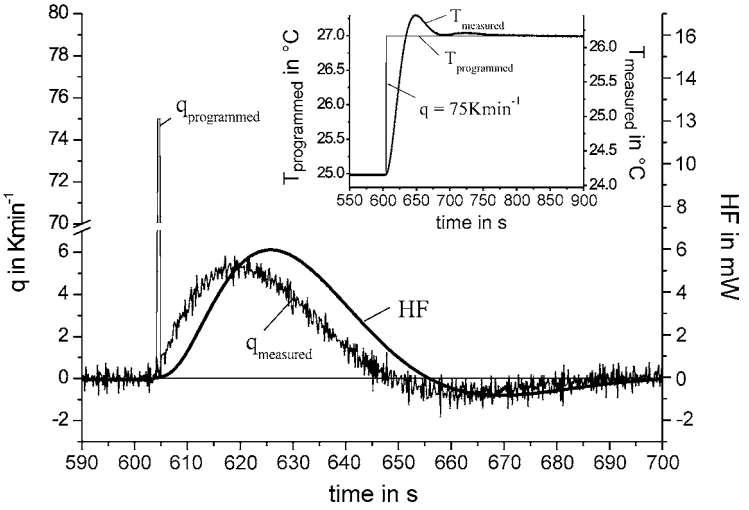

Fig. 3. Heating rate $q_{\text{programmed}}(t)$ and $q_{\text{measured}}(t)$ and heat flow rate HF(t) versus time for one temperature step. The insert shows programmed and measured temperature, $T_{\text{programmed}}$ and T_{measured}. Heating rate is calculated as time derivative of temperature. TA Instruments DSC 2920, aluminum $m_s = 77$ mg.

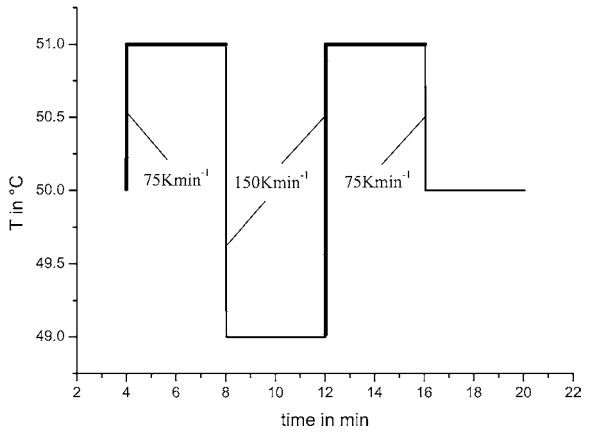

Fig. 4. Temperature–time program of step measurement. The total measuring time of a single step $t_{p\,max} = 4$ min. PerkinElmer Instruments Pyris-1 DSC.

was performed with an empty instrument. Heat flow rate HF(t) of the baseline run was subtracted from that of the sample runs. Further, we analyzed each step in step measurement separately and each TMDSC measurement to calculate $C_{eff}(\omega)$. The results (specific values) are shown in Fig. 5.

For quite different samples, TMDSC and step response analysis give practically the same results. The values of $C_{eff}(\omega)$ from TMDSC lie in between the $C_{eff}(\omega)$ values from heating and cooling steps. This is reasonable since the modulated temperature profile in TMDSC measurements has both heating and cooling parts and results in the average spectrum of $C_{eff}(\omega)$. Some discrepancy between "heating" and "cooling" results (especially remarkable for phase angle at high frequencies) can be assigned to the slightly different behavior of the instrument in heating and cooling mode. Slight non-linearity of the instrument due to limiting cooling capabilities also results in the small difference between the $C_{eff}(\omega)$ values for the two cooling steps. On the contrary, the $C_{eff}(\omega)$ values for the two heating steps coincide better — the instrument behaves linearly within 0.6% even at high frequencies.

One should keep in mind that the presented $C_{eff}(\omega)$ function is not the true heat capacity spectrum of the material. Aluminum as well as polystyrene at 50°C should have frequency independent real valued heat capacity c_p in measured frequency range 0.01–1 rad s^{-1}, which means that modulus Abs($c_p(\omega)$) should be constant and phase angle Arg($c_p(\omega)$) should be zero. Calculated $C_{eff}(\omega)$ corresponds to some effective heat capacity spectrum, which reflects how the transfer function of the instrument-sample system falsifies the true spectrum. $C_{eff}(\omega)$ of the small aluminum disk is mainly influenced by instrumental delay and partly by thermal lag between the disk and DSC furnace. $C_{eff}(\omega)$ of polystyrene disk is influenced by instrumental delay as well, but thermal lag between the disk and DSC furnace makes larger contribution than in case of aluminum disk because of larger mass of polystyrene disk than that of aluminum disk. Poor thermal conductivity of polystyrene shifts the phase angle Arg($C_{eff}(\omega)$) and lowers the modulus

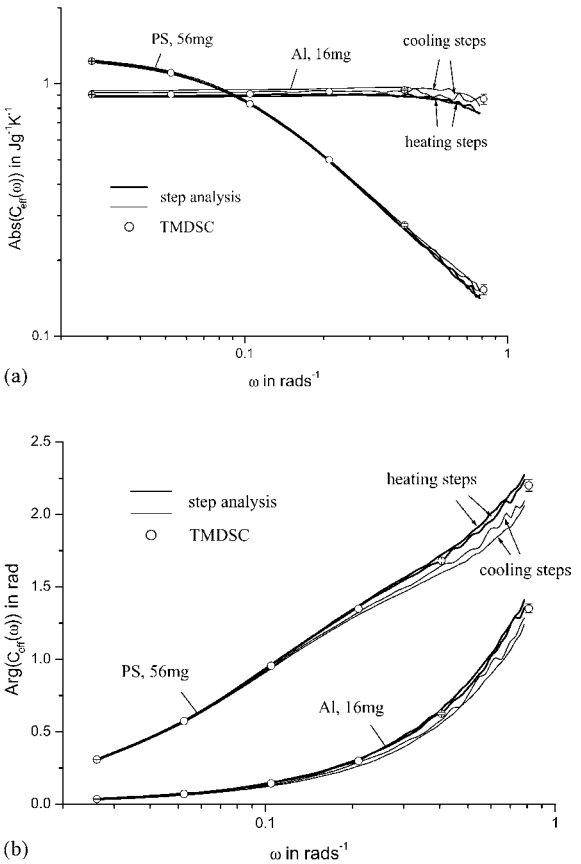

Fig. 5. Modulus Abs($C_{eff}(\omega)$) (a) and phase angle Arg($C_{eff}(\omega)$) (b) of effective specific heat capacity $C_{eff}(\omega)$ of the PS and Al samples versus angular frequency ω calculated by Eq. (2) for two heating and two cooling steps, solid curves. Open circles represent the results of TMDSC measurements. PerkinElmer Instruments Pyris-1 DSC.

Abs($C_{\mathrm{eff}}(\omega)$) in addition. How to determine thermal conductivity of the material from such measurements is described in [7]. The important point of this section is that the effective heat capacity spectra measured by TMDSC or by these single steps are essentially the same.

5. Rate controlled measurements

If one needs to perform a series of similar step measurements (e.g. during scanning of mean temperature), it is not necessary to record the heat flow rate over the whole relaxation time. One can start another step much earlier, see Fig. 6, and consider only a short time interval t_{p}^{*} for the Laplace analysis.

Missing shoulder of the heat flow peak (the part which goes out of the integral limits) is compensated by the presence of shoulders from previous peaks in the integration interval. In case when adjacent peaks have similar shape, Laplace transformation of overlapping peaks ($t_{\mathrm{p}}^{*} < t_{\mathrm{p\,min}}$) results in the same $C_{\mathrm{eff}}(\omega)$ spectrum and $C_{\mathrm{eff}}(0)$ as for a measurement without overlapping ($t_{\mathrm{p}}^{*} \geq t_{\mathrm{p\,min}}$). It is not necessary to keep the time interval between adjacent steps t_{p}^{*} constant. It can slightly differ from step to step depending on the sample response. One can set some criterion to start the next temperature step, e.g. at the moment the heat flow rate returns to steady state within a given limit, let us say one-fifth of the peak height. Then, if a sample relaxes fast one can save time and make the next temperature step. For a slower sample response heat flow rate should be measured over longer time before the next temperature step. If the sample response changes gradually, adjacent peaks of heat flow rate will be similar. This way one can realize rate controlled measurement like in StepScan-DSC$^{\mathrm{TM}}$ and generate $C_{\mathrm{eff}}(\omega)$ spectrum much faster.

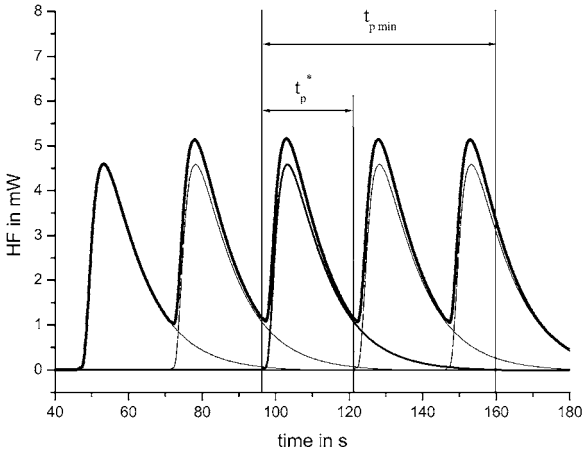

Fig. 6. Calculated example of a heat flow rate, thick curve, consisting of a series of overlapping peaks, thin curves. The minimum relaxation time of each peak (the time the heat flow rate would return back to steady state value after single temperature step) $t_{\mathrm{p\,min}}$ is larger than the time interval between adjacent steps t_{p}^{*}.

6. Discussion

Steady state not necessarily implies isothermal conditions. Step measurements can be performed on top of an underlying scanning of temperature as well. In this case, the heat flow rate at steady state can be far from zero value due to the underlying heating (or cooling). During the time the heat flow rate returns back to the steady state value, this value should not appreciably change. Otherwise, the stationarity condition is not fulfilled. One can also perform step measurements during irreversible processes, e.g. isothermal crystallization. Heat flow rate value in steady state can differ from initial value (the value before the temperature step). How to calculate correctly heat capacity spectrum in this case will be discussed elsewhere [16].

The presented formalism is only correct when the response of the system (apparatus + sample) is linear and stationary [17,18]. To decrease non-linearity, one should decrease the height of the temperature step. To decrease non-stationarity (instrumental drift, evolution of sample properties), one should shorten the length of recorded heat flow relaxation curve if possible. Note that the same restriction on linear and stationary response is valid for TMDSC measurements. From general point of view, there is no preference of one method to another. If we consider real instruments with limiting cooling capabilities, then TMDSC method will face problems to realize large heating rate amplitude, while step analysis with heating steps will be on the safety side. In this situation, TMDSC measurements would have much stronger limitations to keep linear response than step analysis with heating steps. One can conclude this by analyzing results in Figs. 5 and 6.

TMDSC with a lot of repeated periods can be preferable because it gives lower statistical scatter in dynamic heat capacity data than step analysis. On the other hand, step analysis allows generation of continuum heat capacity spectrum, much faster and very easily.

We used in our method steps in temperature to generate as good as possible a heating rate spectrum with the same amplitude for all frequencies. This is an important point since it allows obtaining the heat capacity spectrum with comparable quality at different frequencies. For comparison, steps in heating rate generate heating rate amplitude, which linearly decreases with frequency. The heat capacity spectrum at high frequency has poor quality then. Pulses in temperature, like in the method proposed by Agarwal and Farris [11,12], can generate a very rich heating rate spectrum with amplitudes of high frequency components even exceeding that of low frequency ones. But this can be done only at the expense of large temperature changes, which are not desirable in real measuring conditions. One has to keep temperature changes in some limiting range mainly because of linear response requirements. Then under given limit of temperature changes pulses in temperature will have smaller heating rate amplitude at low frequencies than temperature steps.

7. Conclusion

We proposed a method of step response analysis, which gives practically the same results for frequency dependent complex heat capacity as TMDSC with two advantages: (i) obtaining a continuous heat capacity spectrum and (ii) remarkably shorter measuring time. The measurement consists of a sharp step in temperature followed by an isothermal segment. Measured heat flow rate is evaluated in frequency domain. The method can be applied to any case where the heat capacity spectrum is of interest.

For generation of a heat capacity spectrum with comparable quality at different frequencies, a step in temperature is more preferable than a step in heating rate or pulse in temperature.

Acknowledgements

The work was financially supported by PerkinElmer Instruments, USA. The authors gratefully acknowledge discussions with G.W.H. Höhne.

References

[1] H. Gobrecht, K. Hamann, G. Willers, J. Phys. 4 (1971) 21.
[2] A. Boller, C. Schick, B. Wunderlich, Thermochim. Acta 266 (1995) 97.
[3] A. Toda, T. Oda, M. Hikosaka, Y. Saruyama, Thermochim. Acta 293 (1997) 47.
[4] M. Merzlyakov, A. Wurm, M. Zorzut, C. Schick, J. Macromol. Sci. Phys. 38 (1999) 1045.
[5] W. Hu, T. Albrecht, G. Strobl, Macromolecules 22 (1999) 7548.
[6] B. Wunderlich, R. Androsch, M. Pyda, Y.K. Kwon, Thermochim. Acta 348 (2000) 181.
[7] M. Merzlyakov, C. Schick, Thermochim. Acta 377 (2001) 183.
[8] H. Staub, W. Perron, Anal. Chem. 46 (1974) 128.
[9] J.E.K. Schawe, C. Schick, G.W.H. Höhne, Thermochim. Acta 229 (1993) 37.
[10] J.E.K. Schawe, C. Schick, G.W.H. Höhne, Thermochim. Acta 244 (1994) 49.
[11] N. Agarwal, R.J. Farris, in: Proceedings of the 27th NATHAS Conference, 1999, p. 15.
[12] N. Agarwal, R.J. Farris, Thermochim. Acta 334 (1999) 39.
[13] M. Merzlyakov, C. Schick, Thermochim. Acta 377 (2001) 193.
[14] G.W.H. Höhne, M. Merzlyakov, C. Schick, Thermochim. Acta, submitted for publication.
[15] WWW (internet) URL: http://www.uni-rostock.de/fakult/manafak/physik/poly/.
[16] M. Merzlyakov, C. Schick, in preparation.
[17] M. Merzlyakov, C. Schick, Thermochim. Acta 330 (1999) 55.
[18] M. Merzlyakov, C. Schick, J. Therm. Anal. Calorim. 61 (2000) 649.